Evaluating and predicting the impact of land use and land cover change on land surface temperature in Lac Duong district, Lam Dong province, Vietnam

Phuong T. Nguyen*, Vuong K. Trinh, Hien T. D. Tran, Trinh N. T. Ton, Lan T. T. Nguyen, & Anh N. Nguyen

Faculty of Land Resource and Agricultural Environment, University of Agriculture and Forestry, Hue University, Hue, Vietnam

ARTICLE INFO

Research Paper

Received: August 06, 2024

Revised: October 04, 2024

Accepted: October 07, 2024

Keywords

CA-ANN model

Lac Duong district

Land surface temperature

Land use land cover

Landsat

***Corresponding author**

Nguyen Thuy Phuong

Email: ntphuong.huaf@hueuni.edu.vn

ABSTRACT

Land use and land cover (LULC) change is a key factor influencing land surface temperature (LST) dynamics. This change reflects partly global warming and climate change at local and regional scales. This study aimed to evaluate the effect of LULC on LST change in Lac Duong mountainous district, Lam Dong province in the past 10 years (2013 - 2023), and predict the LST change in 2030. The study used satellite image data from Landsat 8 and 9 OLI to build LULC and LST maps and used the CA-ANN model to predict the LST map. The results showed that the forest land had the LST below 25°C, with the below 20°C LST area correlated negatively with the forest land area, while 20 - 25°C LST correlated positively, especially at the temperature of 22 - 25°C (R^2 = 0.97). The 22 - 25°C and 30 - 35°C temperature levels (R^2 = 0.76 and R^2 = 0.86) correlated sharply with the crop land area. The LST levels between 30 - 40°C reflected the built-up land and bare land with the highest correlation of R^2 = 0.68 and 0.88, respectively. The LST level 20 - 22°C represented the water body area (R^2 = 0.87). The LULC changes had an impact on the LST change in the past 10 years in Lac Duong district. While the forest land area decreased slightly by 0.5%, the cool LST area fell considerably by 10.5% compared to 10 years ago. An almost doubling of the cropland area also led to a doubling in the 25 - 35°C LST areas. In addition, the 35 - 40°C LST level started to happen in several regions. The LST change was predicted to keep increasing in 2030. The temperature was predicted to increase by 2 - 3°C with a maximum temperature of 42°C.

Cited as: Nguyen, P. T., Trinh, V. K., Tran, H. T. D., Ton, T. N. T., Nguyen, L. T. T., & Nguyen, A. N. (2024). Evaluating and predicting the impact of land use and land cover change on land surface temperature in Lac Duong district, Lam Dong province, Vietnam. *The Journal of Agriculture and Development* 23(Special issue 1), 139-154.

1. Introduction

Changes in land use and land cover (LULC) impact directly on the surface biomass - the largest source and sink of terrestrial carbon (Pan et al., 2011), which helps to balance atmospheric CO_2. Therefore, LULC is one of the main drivers for limiting global warming and other aspects of climate change (Sudhakar & Kameshwara, 2010). Land surface temperature (LST) is the skin temperature of the ground derived from solar radiation (Li et al., 2023). The LST measures the radiative temperature of the vegetation canopy and the ground (Weng et al., 2004; Carrillo-Niquete et al., 2022). The LST is a crucial geophysical parameter of climate and biosphere related to surface energy, ecosystem health, and agricultural production (Bhunia et al., 2021; Li et al., 2023). Global temperature varies from -25 to 45°C (NASA, 2024). Monitoring LST dynamics helps assess atmosphere-land surface exchange processes in models and provides valuable surface condition data when combined with other physical properties such as vegetation and soil moisture (ESA, 2024). Land surface temperature is directly affected by LULC.

The LULC change is an inevitable activity of urbanization and socio-economic development. It has been happening worldwide (Rahman et al., 2017; Chang et al., 2018; Baig et al., 2022) and in Vietnam (Trinh & Cao, 2014; Hoang, 2016; Lai & Pham, 2018), leading to an increase in LST at the regional and global scales. Nyatuame et al. (2023) assessed an increase in settlement and cropland in the past and predicted a decrease in crop land and vegetation cover in Ghana in 2030 and 2050. Selmy et al. (2023) used Landsat images and CA-Markov Hybrid to analyze and predict LULC changes in arid regions. The results indicated that the accuracy of LULC categories was quite high with Kappa coefficients > 0.7. The simulation of the future LULC trends to 2050 was increasing urban and crop land.

Increasing temperature occurs not only in urban areas but also in rural and mountainous areas. However, research on LST changes in these areas is still limited. Assessing the impacts of LULC changes on LST changes helps to predict the increasing trend of LST. Thus, managers can evaluate past decisions, and better understand the impacts of current decisions before implementation (NOAA, 2024). It helps managers develop strategies to balance conservation, and handling conflicts between usage and development pressures. LULC and LST maps can be produced by satellite imagery data. Seyam et al. (2023) identified LULC using remote sensing and GIS approach in Mymensingh, Bangladesh with good accuracy from 87.2% to 89.6%.

Lam Dong is located in the Central Highlands and has favorable climate and land conditions for agricultural and forestry development and tourism development. However, Lam Dong is facing some environmental problems related to urban planning and development, deforestation, and landscape destruction. As a mountainous district in the north of Lam Dong, Lac Duong has forest land accounting for 89% of the total natural area, thus, it plays a major role in regulating the climate and creating landscapes for the whole province. The massive use of greenhouse systems on agricultural and forestry lands, and land use change are becoming more and more complicated in Lac Duong district. Therefore, to provide a more scientific basis and properly assess the ongoing negative environmental impacts, this study aims to assess the impact of LULC changes on LST in Lac Duong district during the 2013 - 2023 period and forecast LST changes in 2030.

2. Materials and Methods

2.1. Study site and data

Lac Duong district has administrative boundaries of 5 communes and one town including Lac Duong town, Lat commune, Da Sar commune, Da Nhim commune, Da Chais commune, and Dung K'No commune. It has a temperate climate with temperatures ranging from 11 - 27°C and an average total rainfall of 1,700 - 1,800 mm, so it is mild and cool all year round. High mountain terrain (> 1,600 m) accounts for about 80 - 85% of the natural area of the whole district (PCLDD, 2023). The position of Lac Duong district in Lam Dong province is shown in Figure 1.

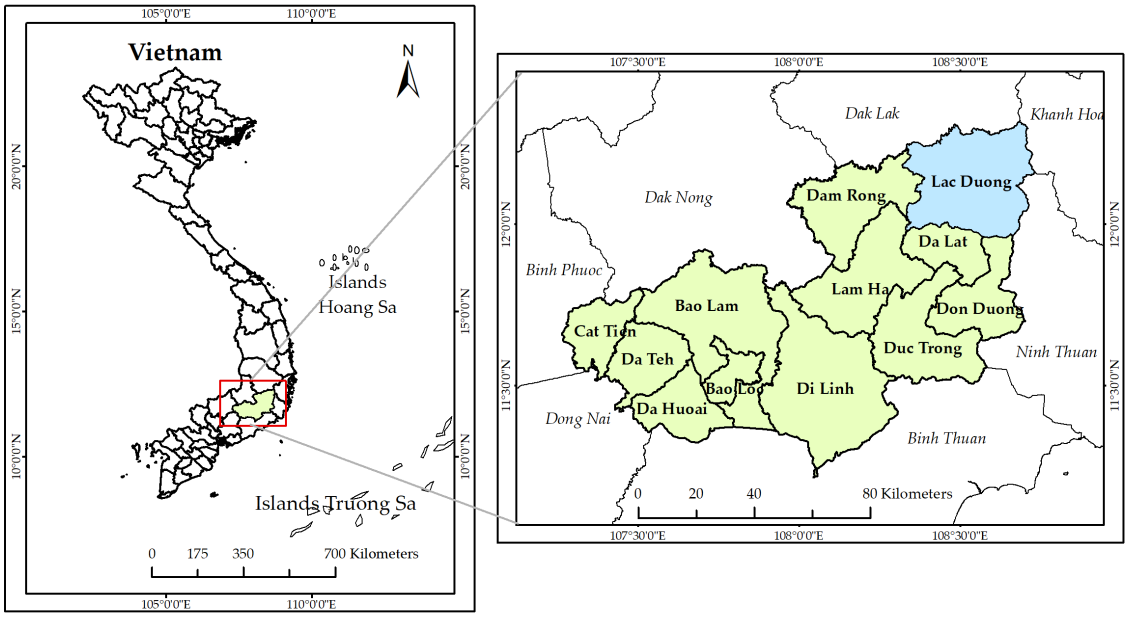

Figure 1. The geographical location of Lac Duong district.

Landsat 8 and 9 OLI satellite imagery data were downloaded from the United States Geological Survey - USGS website. Two satellite imageries (124/051 and 124/052) captured in May 2013 and in March 2015, 2017, 2019, 2021, and 2023 are used to build LULC and LST maps in this study. The satellite imageries meet cloudy conditions (< 10%) and have a spatial resolution of 30 x 30 m.

2.2. LULC and LST maps

2.2.1. LULC map

This study classifies land use and land cover into five types: Forest land, Crop land, Built-up land, Bare land, and Water body. LULC maps are constructed from satellite image data sources combined with a supervised classification method - Maximum Likelihood Classification (MLC) algorithm. The MLC method constructs probability density functions for each class. Each class is characterized by two features including mean vector and covariance matrix, from which the statistical likelihood is calculated for each class. The algorithm will then identify each remaining pixel and will be assigned to the class that it is most likely to be a member of according to the Bayesian formula (Sun et al., 2013).

$$M_k(x) = \ln \mathrm{P}(G_k) + \ln \frac{|S_k^{-1}|^{1/2}}{2\pi^{m/2}} - \frac{1}{2}(x-\mu_k)^T S_k^{-1}(x-\mu_k) \quad (1)$$

Where, is the vector of each pixel; is the likelihood function of x belonging to class k; and are the vector and covariance matrix of class k.

2.2.2. LST map

The LST is calculated using spectral reflectance and correction formulas depending on the image type. The process includes six computation steps: Top of Atmospheric (TOA) spectral radiance, TOA to Brightness Temperature conversion, NDVI, the proportion of vegetation, Emissivity, and Land Surface Temperature. Its formula can be shown as follows (Sajib et al., 2020):

$$LST = \frac{C_2}{\lambda_{eff,TIR10} \cdot ln\left(\frac{C_1 \cdot \tau_{TIR10} \cdot LSE_{TIR10}}{\lambda_{eff}^5 \cdot (L_{TOA10} - L_{up} - \tau_{TIR10}(1-LSE_{TIR10}) \cdot L_{down})} + 1\right)} \quad (2)$$

Where, is the effective wavelength of band Thermal Infrared (TIR); is the Top-of-Atmosphere thermal radiance; is the band TIR average atmospheric transmittance; is the emissivity of the band TIR; C_1 and C_2 are Planck's first and second radiation constants (C_1 = 1.19104 x 10^8 W mm^4 m^{-2} sr^{-1} and C_2 = 1.43877 x 10^4 mm K); L_{up} and L_{down} are the upwelling and downwelling radiance in the atmosphere obtained in band TIR.

2.2.3. Map accuracy assessment

The accuracy of the LULC maps was evaluated using the Kappa coefficient (K) according to the formula 3 (Cohen, 1960). This coefficient presents the measurement of rater reliability, which is computed based on the error matrix of the class identified at 500 randomly selected plots, which were created by Create Random Points in ArcToolbox in ArcMap.

$$K = \frac{N\sum_{i=1}^{r} x_{ii} - \sum_{i=1}^{r}(x_{i+} \cdot x_{+i})}{N^2 - \sum_{i=1}^{r}(x_{i+} \cdot x_{+i})} \quad (3)$$

Where, r - the number of rows in matrix; x_{kk} - the number of observations in row i and column i respectively; x_{i+} and x_{+i} - the total number of samples in row i (positive error) and total number of samples in column i (negative error), respectively; N - the total number of observations.

The coefficient K < 0.40 is low accuracy, 0.41 - 0.60 is moderate accuracy; 0.61 - 0.80 is substantial accuracy, and > 0.81 is perfect accuracy (Li, 2010).

For LULC maps, the study compared the classification results using the MLC method and real classification, which is examined based on the high-resolution images from Google Earth (Islami et al., 2022; Mehra & Swain, 2024).

The accuracy of LST maps built on remote sensing data can be assessed by three methods: temperature-based (T-based), radiance-based (R-based), and cross-validation (Li et al., 2013). Nevertheless, due to the restrictions of time and research finance, this study could not assess the accuracy using the three methods mentioned. Therefore, the reliability of the LST maps is based on the high accuracy of several published studies (Kafy et al., 2021; Onačillová et al., 2022; Nugraha et al., 2024).

2.3. LST prediction

The study uses the Cellular Automata - Artificial Neural Network (CA-ANN) model to predict LST changes by analyzing the trends of land surface temperature changes. The CA-ANN model is a combination of the spatial operation of the cellular automata model and the artificial neural network system. The prediction of LST changes uses three types of input data: (1) NDVI fluctuations over the years; (2) LST data transfer matrix; and (3) land use planning in 2030. This model is run on the MOLUSCE plugin software in QGIS 2.8.9.

The analysis results of LST changes in the period 2015 - 2023 are a basis for predicting LST map in 2030. To ensure the reliability of predictive modelling, the study was first used the CA-ANN model to estimate the LST map in 2023, and then evaluated the accuracy of this map by comparing it with the LST map calculated from remote sensing images through the Kappa coefficient.

3. Results and Discussion

3.1. LULC changes

The LULC maps from 2013 to 2023 are shown in Figure 2. The LULC maps built had high and very high accuracy with the Kappa coefficients ranging from 0.76 to 0.85 (Table 1). The Kappa coefficients of the LULC maps were approximately the same as some published studies using different satellite image data sources. Specifically, the study by Islami et al. (2022) constructed LULC maps in Sadar Watershed, Mojokerto Regency, Indonesia using Landsat 5 and Sentinel-2 images, with Kappa coefficients ranging from 0.74 - 0.80. Therefore, they are suitable and reliable for assessing the LULC changes in Lac Duong district.

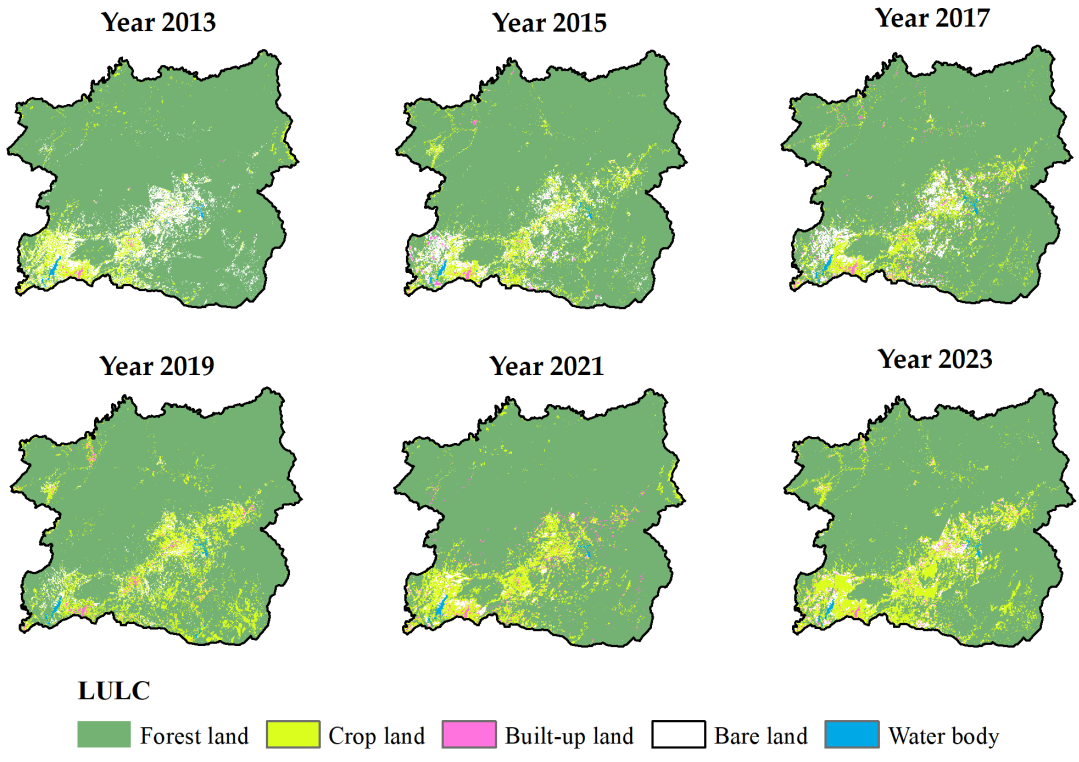

Figure 2. Land use and land cover (LULC) maps from 2013 to 2023.

Table 1. Error matrix and accuracy of land use and land cover classification

Year	ClassValue	C_1	C_2	C_3	C_4	C_5	Total	U_Accuracy	Kappa
2013	C_1	432	0	0	0	0	432	1	0
	C_2	16	33	1	4	0	54	0.61	0
	C_3	2	1	5	0	0	8	0.63	0
	C_4	0	0	0	5	0	5	1	0
	C_5	0	0	0	0	1	1	1	0
	Total	450	34	6	9	1	500	0	0
	P_Accuracy	0.96	0.97	0.83	0.56	1	0	0.95	0
	Kappa	0	0	0	0	0	0	0	0.78
2015	C_1	404	4	0	1	0	409	0.99	0
	C_2	3	32	0	2	0	37	0.86	0
	C_3	0	0	1	0	0	1	1	0
	C_4	4	9	3	36	0	52	0.69	0
	C_5	0	0	0	0	1	1	1	0
	Total	411	45	4	39	1	500	0	0
	P_Accuracy	0.98	0.71	0.25	0.92	1	0	0.95	0
	Kappa	0	0	0	0	0	0	0	0.83
2017	C_1	426	0	0	0	0	426	1	0
	C_2	7	26	1	4	0	38	0.68	0
	C_3	1	0	2	0	0	3	0.67	0
	C_4	1	5	0	27	0	33	0.82	0
	C_5	0	0	0	0	0	0	0	0
	Total	435	31	3	31	0	500	0	0
	P_Accuracy	0.98	0.84	0.67	0.87	0	0	0.96	0
	Kappa	0	0	0	0	0	0	0	0.85
2019	C_1	406	4	2	12	0	424	0.96	0
	C_2	8	34	0	4	0	46	0.74	0
	C_3	0	0	4	1	0	5	0.80	0
	C_4	0	3	0	22	0	25	0.88	0
	C_5	0	0	0	0	0	0	0	0
	Total	414	41	6	39	0	500	0	0
	P_Accuracy	0.98	0.83	0.67	0.56	0	0	0.93	0
	Kappa	0	0	0	0	0	0	0	0.76

2021	C_1	374	9	0	5	0	388	0.96	0
	C_2	10	64	2	7	0	83	0.77	0
	C_3	0	1	4	0	0	5	0.80	0
	C_4	0	0	0	23	0	23	1	0
	C_5	0	0	0	0	1	1	1	0
	Total	384	74	6	35	1	500	0	0
	P_Accuracy	0.97	0.86	0.67	0.66	1	0	0.93	0
	Kappa	0	0	0	0	0	0	0	0.82
2023	C_1	406	10	0	7	0	423	0.96	0
	C_2	4	37	1	5	0	47	0.79	0
	C_3	0	0	2	1	0	3	0.67	0
	C_4	0	3	0	23	0	26	0.88	0
	C_5	0	0	0	0	1	1	1	0
	Total	410	50	3	36	1	500	0	0
	P_Accuracy	0.99	0.74	0.67	0.64	1	0	0.94	0
	Kappa	0	0	0	0	0	0	0	0.79

C_1: Forest land, C_2: Crop land, C_3: Built-up land, C_4: Bare land, C_5: Water bodies.

Table 2. The areas of land use and land cover (LULC) types from 2013 to 2023

Index	LULC	2013	2015	2017	2019	2021	2023
Area (km^2)	Forest land	1085.31	1087.00	1084.51	1080.64	1080.10	1080.41
	Crop land	65.29	72.70	75.84	96.05	109.81	122.95
	Built-up land	23.36	24.06	24.94	25.41	26.90	26.27
	Bare land	89.68	81.57	79.80	62.51	47.67	35.10
	Water body	4.78	3.11	3.34	3.81	3.95	3.70
	Total	1268.43	1268.43	1268.43	1268.43	1268.43	1268.43

The areas of five land uses/land cover types are presented in Table 2. The total area of Lac Duong district was 1,268.4 km^2, of which forest land accounted for the majority, with about 85%. From 2013 to 2019, the forest land area decreased by about 6.4 km^2 (about 0.6% of the forest area) from 1,087.0 km^2 to 1,080.64 km^2 before remaining stable until 2023. The decrease in forest land area might be due to land-hiring companies and enterprises building a large number of greenhouses on the forest land. These areas are still forest land, yet remote sensing image interpretation and the MLC model identify them as croplands. In the following years, local authorities proceeded to dismantle greenhouses built on forest land, so the forest land area began to gradually increase again. The changing trends of crop land and bare land were quite evident in the past 10 years. The area of crop land nearly doubled from 65.29 to 122.95 km^2. In contrast,

the area of bare land decreased considerably by 61% from 89.68 km^2 to 35.10 km^2. The results of the change in the built-up land area indicated that the urbanization rate has slightly increased in Lac Duong district. After 10 years, the area of built-up land increased by about 3 km^2 (about 12.5% of this land use) to 26.67 km^2. Another land use type that was also relatively stable over time was the water body area. The slight fluctuation of this cover could be mainly due to rainfall at the time of taking the images because there was no water surface area leveling for construction and other purposes.

In short, the crop land and built-up land areas tended to rise gradually, meanwhile, the bare land area decreased in the period 2013 - 2023.

3.2. LST changes

The LST maps of years are shown in Figure 3. The surface temperature was classified into 8 levels and their areas are listed in Figure 4. The research results indicated that the low-temperature levels below 25°C were distributed in forest land, accounting for most of the district's area, ranging from 78.1% to 88.9%. This area peaked in 2013 (88.9%) and reached its lowest points in 2023 and 2015 at 79.2% and 78.1%, respectively. The areas of LST levels above 25°C presented mainly cropland, built-up land, and bare land. This could be observed on the LST maps. The temperature levels above 25°C occupied 11.2 - 21.1% of the total area of the district in the past 10 years.

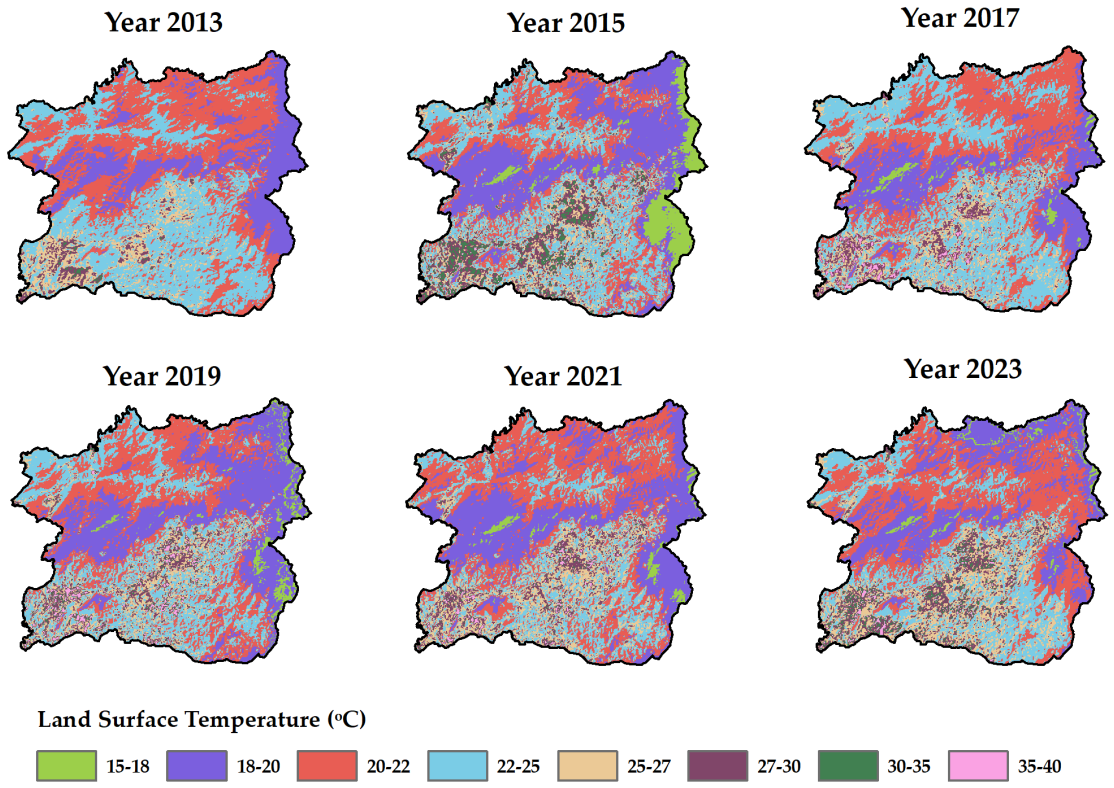

Figure 3. Land surface temperature maps from 2013 to 2023.

The LST change shows the trends over time: First, the LST difference in the district was from 15 to 40°C since 2015, higher than in 2013 (18 - 35°C). Second, the LST level above 30°C generally had a considerable increase from 3.2 km^2 to 33.1 km^2, a 7-fold increase after ten years. Third, the LST distribution in 2015 was different from other years. The areas with LST levels 15 - 18°C and 27 - 40°C were significantly larger. It could be directly related to the normalized difference vegetation index (NDVI). In 2015, the area with a low NDVI (0.15 < NDVI < 0.23) was significantly higher than those in other years, leading to an increase in the hot temperature area (27 - 40°C). In contrast, the area with a high NDVI index (0.34 < NDVI < 0.5) in this year was significantly lower than those in other years, leading to a decrease in the cool temperature area (15 - 18°C). LST changes can be influenced by factors such as land use and land cover, natural biogeography, background climate, radiation intensity, thermal resistance, evapotranspiration, soil heat flux and air temperature (Kummari et al., 2022; Patel et al., 2024). In this case study, satellite images were caught very close to each in the studied years, so the climate difference was minimized. Therefore, the LST changes over the years were mainly related to land use, land cover changes. The lowest temperature could be influenced by the NDVI index and the highest temperature was influenced by the built-up land.

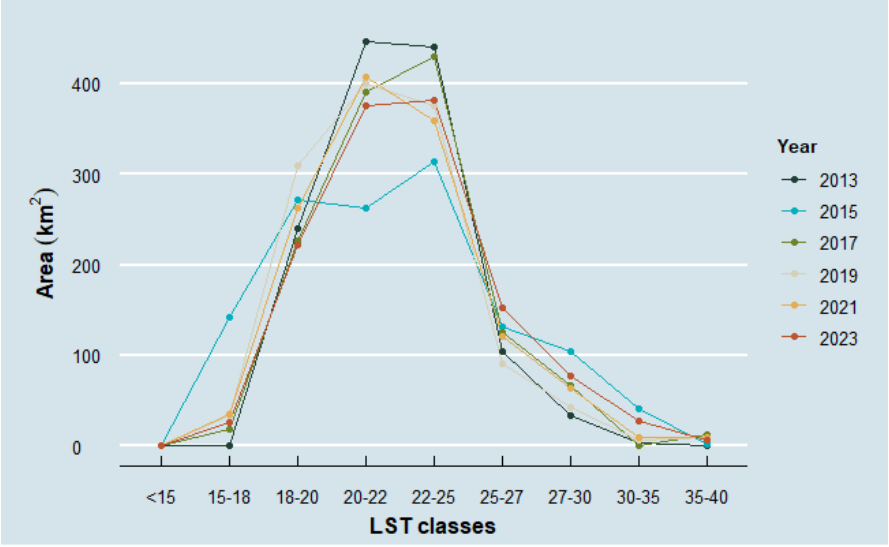

Figure 4. The areas of land surface temperature (LST) classes in 2013 - 2023.

This LST increase was also consistent with the ongoing global warming trend in the world. The LST increasing trend in Lac Duong was similar to that of the global. The global average surface temperature increased by 1.36°C, warmer than the pre-industrial standard (1850 - 1900) used to measure global warming (Nasa, 2023). A study by Tian et al. (2023) in Nanjing City, China also gave similar results but with a lower rate of LST increase than Luoyang County, within 30 years (1990 - 2020), the average LST increased by 2.24°C.

The LST distribution has been tending to go up to temperature and increase the area of higher temperatures over the past 10 years.

3.3. Effects of LULC on LST

Land surface temperature reflects the solar radiation energy of the land surface, so land surface characteristics such as vegetation index, topographic elements, soil moisture, water, land use type, land cover are very important factors affecting LST. The study assessed the impact of LULC changes on LST by evaluating the correlation between the area of a LULC type and the areas of eight LST levels (15 - 18°C, 18 - 20°C, 20 - 22°C, 22 - 25°C, 25 - 30°C, 30 - 35°C, and 35 - 40°C). The area of the temperature level that shows a sharp correlation with a LULC type, then that LST level reflects the characteristics of corresponding LULC.

Forest land exhibited LST levels below 25°C, and agricultural land, built-up land, and bare land represented LST levels ranging from 25 to 40°C. Thus, the impact of LULC changes on LST changes was rated accordingly (Figure 5). In addition, due to a considerable difference in NDVI, the data in 2015 was not included in the correlation assessment.

The results indicated that forest land area had an obvious negative correlation with LST levels 15 - 18°C (R^2 = 0.81) and 22 - 25°C (R^2 = 0.97). Meanwhile, the areas with LST levels 18 - 22°C had an unobvious correlation with the forest land. The forest quality like forest health and biomass density is a key factor affecting the lower temperature levels (15 - 18°C, 18 - 20°C, and 20 - 22°C). The denser the forest biomass is, the higher and denser the forest biomass is, the lower the LST is. Thus, the total forest area did not show a clear positive correlation with the lower-temperature levels (from 15°C to 22°C), even showing a negative correlation. The very good negative correlation of forest land area with the 15 - 18°C temperature zone (R^2 = 0.81) may be due to the fact that the total forest land area increases but the area with very dense biomass decreases. On the other hand, the forest land with moderate biomass could reflect the temperature of 22 - 25°C, so the LST levels had a fairly good correlation with the total forest area. Forests have dense vegetation which has the great adsorption capacity of solar radiation. Vegetation has the ability to 80% of incoming visible radiation, reflecting 10% and transmitting 10% (Shahidan et al., 2006). Thus, the forest land reflected the lowest LST. The result indicated that the forest area has decreased by only 0.5%, yet the LST level below 25°C has decreased by 10.5% over the past 10 years.

For crop land, the areas with LST levels of 22 - 35°C increased significantly when this land use type increased. This land use type correlates better with the 22 - 25°C and 30 - 35°C temperature levels (R^2 = 0.76 and R^2 = 0.86). Although the agricultural land was covered good vegetation (just behind the forest), the use of a large number of greenhouses in recent years in Lac Duong district has increased the surface temperature for this land cover. According to local government's report, Lac Duong has 1,648 ha of greenhouses in 2023, an increase of 182 ha compared to 2022. The materials of greenhouses increased the reflection of incoming solar radiation. An approximate doubling of the area of this LULC type also nearly doubled the 25 - 35°C LST area. A study on cropland in Yayo district, in Ethiopia also showed that the average LST on this land use type increased from 22.8°C in 1986 to 27 °C in 2003 by Moisa et al. (2023), which was identified as due to climate change.

The built-up land indicated a better correlation with the high-temperature area. The LST levels 27 - 40°C reflected built-up land. In particular, the

35 - 40°C level correlated the best with the built-up land (R^2 = 0.68). This land use type had high temperatures due to properties of construction materials (concrete, stone, asphalt...) which has high thermal conductivity and absorbs heat well and quickly, thus heating the surface quickly. In addition, due to poor water permeability and limited water evaporation, heat energy is retained on the surface of the material much higher and longer than in areas with green trees or wet soil. Zhang et al. (2023) also evaluated that the urban lands had the LST > 30°C. From the analysis of satellite data from 1992 to 2020, Jagtap et al. (2024) found that expanding construction areas caused a significant temperature increase of 4.3°C in built-up areas in Pakistan.

Meanwhile, the water body area indicated a sharp correlation with the LST level 20 - 22°C (R^2 = 0.87). For bare land, this land cover type had a very sharp correlation with the LST level 30 - 35°C (R^2 = 0.88), and lower correlations with the LST levels 27 - 30°C and 35 - 40°C (R^2 = 0.49 and 0.43, respectively). The water surfaces, despite their low thermal response, are known to be the best absorbers of radiation and provide evaporative cooling where water evaporates as solar radiation reaches the water surface and removes heat, cooling surrounding features. Increasing water accessibility increased evaporation, providing additional cooling during the day.

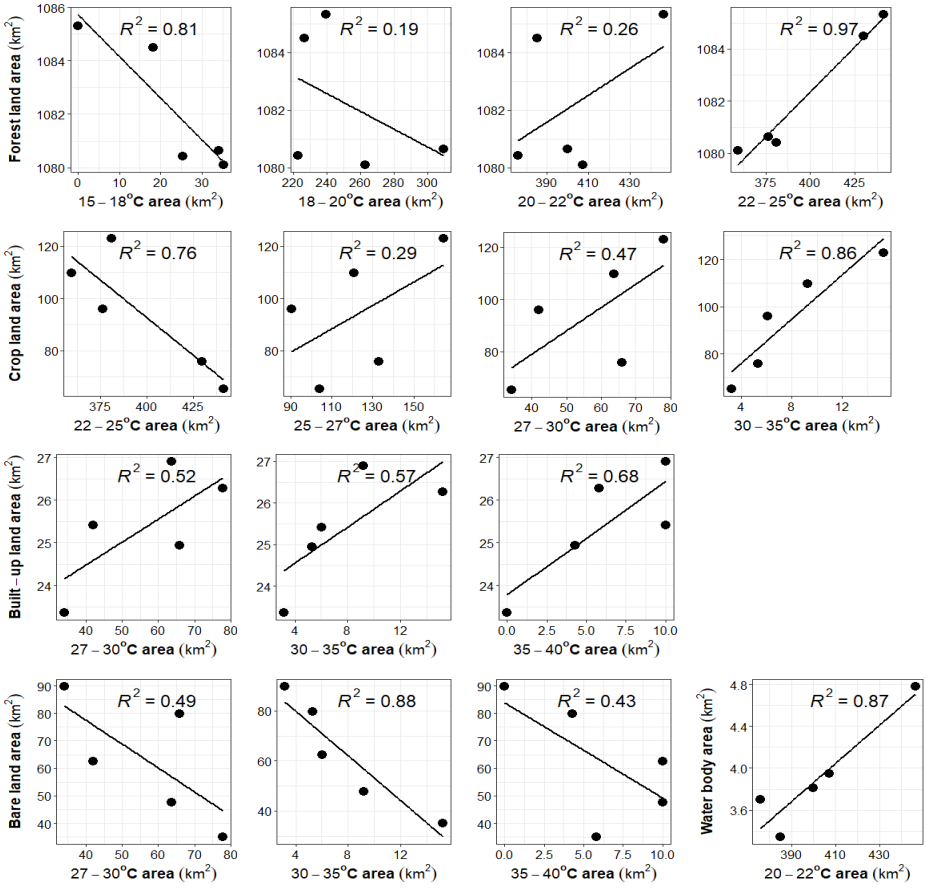

Figure 5. Correlation between areas of land use and land cover type and area of land surface temperature class.

In summary, the LST level 30 - 35°C had a better correlation with cropland area than with built-up land (R^2 = 0.86 and R^2 = 0.57). This result reflected the significant increase in the number of greenhouses in agricultural production, leading to the surface temperature increase of cropland in Lac Duong district over the past 10 years. The cropland increased 1.1 times in 2023 compared to 2021, and nearly 2 times compared to 10 years ago. Meanwhile, the LST level 30 - 35°C increased 1.7 times in 2023 compared to 2021, about 2.5 times compared to 2019, and about 5 times after 10 years. According to the local government report, Lac Duong district had nearly 0.24 km^2 of greenhouses in 2022. Although the total area of built-up land and bare land decreased considerably to one-third, from 178.3 km^2 to 61.3 km^2, the areas with high-temperature (30 - 40°C) still increased about 6.5 times, from 3.19 km^2 to 21.07 km^2 after 10 years.

3.4. LST prediction

The mentioned assessment indicated that the LST change in Lac Duong was affected by three main factors, which are the basis for predicting the LST map in 2030. Firstly, forest biomass (represented by the NDVI index) was an important factor affecting the LST change in low-temperature areas. Except for 2015, the NDVI on forest land remained relatively stable. Therefore, the study used the fluctuations of the NDVI map for the remaining years to create a LST forecast map. Secondly, using greenhouses in agricultural production was one of the causes of the increase in LST level 30 - 35°C. However, the local government is gradually dismantling 19 hectares of greenhouses on forestry land, and restricting farmers from using greenhouses the next time. Third, the study is based on the Land Use Planning map to 2030 of Lac Duong district according to Decision No. 1869/QD-UBND as the basis for predicting the 2030 LST map (PCLDD, 2023).

To ensure the reliability of the predicted LST map, the study evaluated the accuracy of the simulated 2023 LST map. The 2023 LST map was estimated by the CA-ANN model shown in Figure 6. The accuracy of this simulated map when compared with the 2023 LST map calculated by remote sensing images gave a Kappa coefficient of 0.73. Therefore, this algorithm met the reliability for predicting the 2030 LST map.

The predicted 2030 LST map and the area statistics of the LST levels are shown in Figure 6. The forecast results indicated that LST was expected to continue to increase by 2 - 3°C, ranging from 15°C to 42°C. The low-temperature area was predicted to decrease gradually and the high-temperature area continued to increase. The LST level of 15 - 25°C tended to decrease compared to 2023, especially the area of 15 - 18°C decreased to only one-fifth of its area in 2023. The LST levels from 25 to 40°C were forecasted to increase considerably. In addition, the area with LST level 40 - 42°C was predicted to appear.

Although the limitation of greenhouse use in local agricultural production has a positive impact on LST, land use change could continue to increase the temperature in the future. Therefore, in addition to measures to limit the use of greenhouses and reforestation local authorities should combine measures to improve forest quality (increase biomass and forest health) and restrict bare land. In addition, urban planning should focus on increasing green spaces in urban

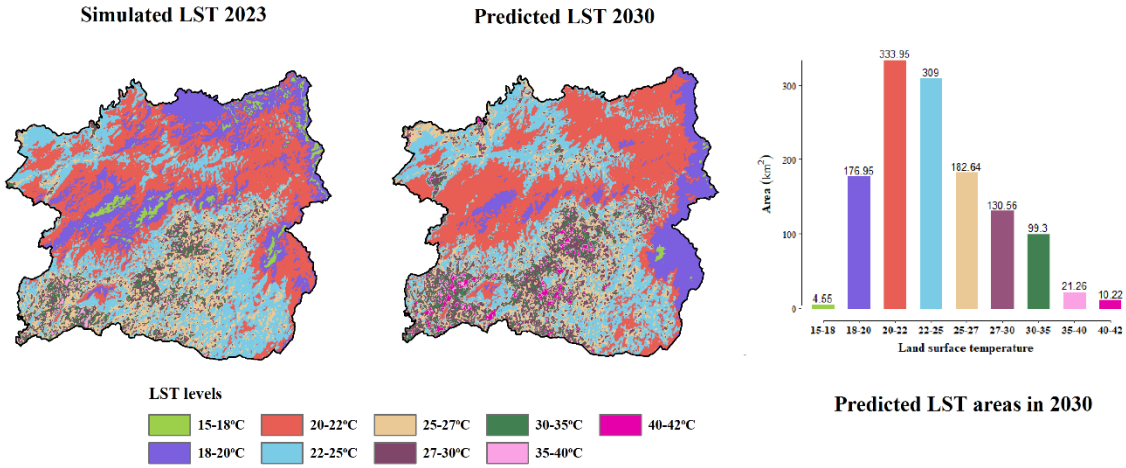

areas to reduce the increase in surface temperature on built-up land.

Figure 6. Simulated and predicted land surface temperature (LST) maps in 2023 and 2030, and LST statistics in 2030.

4. Conclusions

Forest land reflected the temperature below 25°C. Forest land area correlated with the LST 22 - 25°C. Water land mainly reflected temperature levels of 20 - 22°C. The cropland ranged from 25 to 35°C. Built-up and bare lands reflected the temperature level of 30 - 40°C, in which the highest temperature area represented built-up land. The LULC changes significantly affected the LST changes in the past 10 years in Lac Duong district. Even though the forest area decreased slightly by only 0.5%, the low-LST area below 25°C reduced considerably by 10.5% due to decreased forest quality. An almost doubling of the cropland area also led to doubling the 25 - 35°C area doubling. The area of 30 - 40°C LST levels increased over ten times due to increasing the built-up land area by 12.5%. In addition, a high temperature of 35 - 40°C appeared in this period.

The study predicted the LST change trend in 2030. The results revealed that LST would continue to increase in 2030 with temperature fluctuations ranging from 15 - 42°C. The lower temperature areas (below 25°C) was predicted to decrease and the higher temperature areas (35 - 42°C) to increase. Some factors like satellite image sources may improve the accuracy of LST maps that this study has not evaluated. Therefore, future studies should focus on the application of more different satellite image sources and other prediction models.

Conflict of interest

The authors declare no conflict of interest. The funders had no role in the design of the study; in the collection, analyses, or interpretation of data; in the writing of the manuscript; or in the decision to publish the results.

Acknowledgements

We sincerely thank University of Agriculture and Forestry, Hue University for helping throughout the research process.

References

Baig, M. F., Mustafa, M. R. U., Baig, I., Takaijudin, H. B., & Zeshan, M. T. (2022). Assessment of land use land cover changes and future predictions using CA-ANN simulation for Selangor, Malaysia. *Water* 14(3), 402. https://doi.org/10.3390/w14030402.

Bhunia, G. S., Chatterjee, U., Kashyap, A., & Shit, P. K. (2021). *Land reclamation and restoration strategies for sustainable development: geospatial technology based approach* (1st ed.). Amsterdam, The Netherlands: Elsevier.

Carrillo-Niquete, G. A., Andrade, J. L., Valdez-Lazalde, J. R., Reyes-García, C., & Hernández-Stefanoni, J. L. (2022). Characterizing spatial and temporal deforestation and its effects on surface urban heat islands in a tropical city using Landsat time series. *Landscape and Urban Planning* 217(4), 1-13. https://doi.org/10.1016/j.landurbplan.2021.104280.

Chang, Y., Hou, K., Li, X., Zhang, Y., & Chen, P. (2018). Review of land use and land cover change research progress. *IOP Conference Series: Earth and Environmental Science* 113, 012087. https://doi.org/10.1088/1755-1315/113/1/012087.

Cohen, J. (1960). A coefficient of agreement for nominal scales. *Educational and Psychological Measurement* 20(1), 37-46. https://doi:10.1177/001316446002000104.

ESA (European Space Agency). Land surface temperature. (2024). Retrieved July 16, 2024, from https://climate.esa.int/en/projects/land-surface-temperature/.

Hoang, A. H. (2016). A study on land surface temperature (LST) from landsat 8 TIRS - a case study of Thai Nguyen city. *Journal of Hydrometeorology* 10(670), 26-32.

Islami, F. A., Tarigan, S. D., Wahjunie, E. D., & Dasanto, B. D. (2022). Accuracy assessment of land use change analysis using google earth in sadar watershed mojokerto regency. *IOP Conference Series: Earth and Environmental Science* 950, 012091. https://doi.org/10.1088/1755-1315/950/1/012091.

Jagtap, A. A., Shedge, D. K., & Mane, P. B. (2024). Exploring the effects of land use/land cover (LULC) modifications and land surface temperature (LST) in Pune, Maharashtra with anticipated LULC for 2030. *International Journal of Geoinformatics* 20(2), 42-62. https://doi.org/10.52939/ijg.v20i2.3065.

Kafy, A. A., Dey, N. N., Rakib, A. A., Rahaman, Z. A., Nasher, N. M. R., & Bhatt, A. (2021). Modeling the relationship between land use/land cover and land surface temperature in Dhaka, Bangladesh using CA-ANN algorithm. *Environmental Challenges* 4, 100190. https://doi.org/10.1016/j.envc.2021.100190.

Kummari, R., Allu, P. K. R., Mesapam, S., Allu A. R., Vinakallu, B., & Ankam, B. P. (2022). Effect of LULC changes on land surface temperature. In Mesapam, S., Ohri, A., Sridhar, V., & Tripathi, N. K (Eds.). *Developments and applications of geomatics* 450, 155-174. Singapore: Springer Nature. https://doi.org/10.1007/978-981-99-8568-5_12.

Lai, T. A., Pham, V. M., & Phạm, M. T. (2018). Quantitative assessment of land use/land cover change through multi-temporal remote sensed data in Dien Bien province, Vietnam. *Journal of Water Resources and Environmental Engineering* 62, 72-29.

Li, X. (2010). *Kappa - A critical review*. Retrieved July 26, 2024, from https://uu.diva-portal.org/smash/get/diva2:326034/FULLTEXT01.pdf.

Li, Z. L., Wu, H., Duan, S. B., Zhao, W., Ren, H., Liu, X., Leng, P., Tang, R., Ye, X., Zhu, J., Sun, Y., Si, M., Liu, M., Zhang, X., Shang, G., Tang, B-H., Yan, G., & Zhou, C. (2023). Satellite remote sensing of global land surface temperature: Definition, methods, products, and applications. *Reviews of Geophysics* 61(1), e2022RG000777. https://doi.org/10.1029/2022RG000777.

Mehra, N., & Swain, J.B. (2024). Assessment of land use land cover change and its effects using artificial neural network-based cellular automation. *Journal of Engineering and Applied Science* 71(1), 70. https://doi.org/10.1186/s44147-024-00402-0.

Moisa, M. B., Gabissa, B. T., Wedajo, Y. N., Gurmessa, M. M., Deribew, K. T., Negasa, G. G., Negassa, M. D., & Gemeda, D. O. (2023). Analyzing the correlation of forest and wetland with land surface temperature by using geospatial technology: a case of Yayo district, Southwestern Ethiopia. *Geocarto International* 38(1), 2256300. https://doi.org/10.1080/10106049.2023.2256300.

NASA (National Aeronautics and Space Administration). (2024). *Land surface temperature*. Washington, USA: National Aeronautics and Space Administration.

NASA (National Aeronautics and Space Administration). (2023). *Global temperature*. Washington, USA: National Aeronautics and Space Administration.

NOAA (National Oceanic and Atmospheric Administration). (2024). *What is the difference between land cover and land use?* Maryland, USA: National Oceanic and Atmospheric Administration.

Nugraha, A. S. A., Kamal, M., Murti, S. H., & Widyatmanti, W. (2024). Accuracy assessment of land surface temperature retrievals from remote sensing imagery: pixel-based, single and multi-channel methods. *Geomatics, Natural Hazards and Risk* 15(1), 2324975. https://doi.org/10.1080/19475705.2024.2324975.

Nyatuame, M., Agodzo, S., Amekudzi, L. K., & Mensah-Brako, B. (2023). Assessment of past and future land use/cover change over Tordzie watershed in Ghana. *Frontiers in Environmental Science* 11, 1139264. https://doi.org/10.3389/fenvs.2023.1139264.

Onačillová, K., Gallay, M., Paluba, D., Péliová, A., Tokarčík, O., & Laubertová, D. (2022). Combining landsat 8 and sentinel-2 data in google earth engine to derive higher resolution land surface temperature maps in urban environment. *Remote Sensing* 14(6), 4076. https://doi.org/10.3390/rs14164076.

Pan, Y., Birdsey, R. A., Fang, J., Houghton, R., Kauppi, P. E., Kurz, W. A., Oliver L. Phillips, O. L., Shvidenko, A., Simon L. Lewis, S. L., Canadell, J. G., Ciais, P., Jackson, R. B., Pacala, S. W., McGuire, A. D., Piao, S., Rautiainen, A., Sitch, S., & Hayes, D. (2011). A large and persistent carbon sink in the world's forests. *Science* 333(6045), 988-993. https://doi.org/10.1126/science.1201609.

Patel, S., Indraganti, M., & Jawarneh, R. N. (2024). A comprehensive systematic review: impact of land use/land cover (LULC) on land surface temperatures (LST) and outdoor thermal comfort. *Building and Environment* 249, 111130. https://doi.org/10.1016/j.buildenv.2023.111130.

PCLDD (People's Committee of Lac Duong District). (2023). Decision No. 1869/QD-UBND dated on September 29, 2023. On approving the land use planning until 2030 of Lac Duong district, Lam Dong province. Retrieved December 10, 2023, from https://thuvienphapluat.vn/van-ban/Bat-dong-san/Quyet-dinh-1869-QD-UBND-2023-quy-hoach-su-dung-dat-huyen-Lac-Duong-Lam-Dong-581702.aspx.

PCLDD (People's Committee of Lac Duong District). (2023). *Report on the results of implementing socio-economic development tasks in 2023*. Lam Dong, Vietnam: People's Committee of Lac Duong District.

Rahman, M. T. U., Tabassum, F., Rasheduzzaman, M., Saba, H., Sarkar, L., Ferdous, J., Uddin, S. Z., & Islam, A. Z. M. Z. (2017). Temporal dynamics of land use/land cover change and its prediction using CA-ANN model for southwestern coastal Bangladesh. *Environmental Monitoring and Assessment* 189(565), 1-18. https://doi.org/10.1007/s10661-017-6272-0.

Sajib, M. Q. U., & Wang, T. (2020). Estimation of land surface temperature in an agricultural region of Bangladesh from landsat 8: intercomparison of four algorithms. *Sensors* 20(6), 1778. https://doi.org/10.3390/s20061778.

Selmy, S. A. H., Kucher, D. E., Mozgeris, G., Moursy, A. R. A., Jimenez-Ballesta, R., Kucher, O. D., Fadl, M. E., & Mustafa, A. A. (2023). Detecting, analyzing, and predicting land use/land cover (LULC) changes in arid regions using landsat images, ca-markov hybrid model, and gis techniques. *Remote Sensing* 15(23), 5522. https://doi.org/10.3390/rs15235522.

Seyam, M. M. H., Haque, M. R., & Rahman, M. M. (2023). Identifying the land use land cover (LULC) changes using remote sensing and GIS approach: A case study at Bhaluka in Mymensingh, Bangladesh. *Case Studies in Chemical and Environmental Engineering* 7, 100293. https://doi.org/10.1016/j.cscee.2022.100293.

Shahidan, M. F., Salleh, D. E., & Shariff, M. K. M. (2006). The influence of tree canopy on the thermal environment in a tropical climate: a preliminary study. *iNTA Conference 2006 - Harmony in Culture and Nature*. Geneva, Switzerland: WIPO. Retrieved July 2, 2024, from https://www.researchgate.net/publication/224054095_The_Influence_of_Tree_Canopy_on_Thermal_Environment_in_a_Tropical_Climate

Sudhakar, S., & Kameshwara S. V. C. R. (2010). Chapter 2: Land use and Land cover Analysis. In P. S. Roy, R. S. Dwivedi, & D. Vijayan (Eds.). *Remote sensing application* (2nd ed., 21-48). Retrieved July 1, 2024, from https://www.nrsc.gov.in/sites/default/files/pdf/ebooks/Chap_2_LULC.pdf.

Sun, J., Yang, J., Zhang, C., Yun, W., & Qu, J. (2013). Automatic remotely sensed image classification in a grid environment based on the maximum likelihood method. *Mathematical and Computer Modelling* 58(3-4), 573-581. https://doi.org/10.1016/j.mcm.2011.10.063.

Tian, L., Tao, Y., Li, M., Qian, C., Li, T., Wu, Y., & Ren, F. (2023). Prediction of land surface temperature considering future land use change effects under climate change scenarios in Nanjing city, China. *Remote Sensing* 15(11), 2914. https://doi.org/10.3390/rs15112914.

Trinh, T. T. H., & Cao T. D. (2014). Change in land use using pre-classification and post-classification. *Journal of Mining and Earth Sciences* 48(10), 58-62.

Weng, Q., Lu, D., & Schubring, J. (2004). Estimation of land surface temperature–vegetation abundance relationship for urban heat island studies. *Remote Sensing of Environmen*t 89(4), 467-483. https://doi:10.1016/j.rse.2003.11.005.

Zhang, M., Kafy, A. A., Xiao, P., Han, S., Zou, S., Saha, M., Zhang, C., & Tan, S. (2023). Impact of urban expansion on land surface temperature and carbon emissions using machine learning algorithms in Wuhan, China. *Urban Climate* 47, 101347 https://doi.org/10.1016/j.uclim.2022.101347.